Scientific paper

# Determination of Oxygen by Means of a Biogas and Gas – Interference Study Using an Optical Tris (4,7-Diphenyl-1,10-Phenanthroline) Ruthenium(II) Dichloride Complex Sensor

**Polonca Brglez,[1,3] Andrej Holobar,[1] Aleksandra Pivec,[2] Nataša Belšak[2,3] and Mitja Kolar[3,4]***

[1] *ECHO d.o.o., Stari trg 37, SI-3210 Slovenske Konjice, Slovenia*

[2] *ZRS Bistra Ptuj, Slovenski trg 6, SI-2250 Ptuj, Slovenia*

[3] *University of Maribor, Faculty of Chemistry and Chemical Engineering, Smetanova 17, SI-2000 Maribor, Slovenia*

[4] *Centre of Excellence PoliMaT, Tehnološki park 24, SI-1000 Ljubljana, Slovenia*

* *Corresponding author: E-mail: mitja.kolar@uni-mb.si, tel. ++386-22294-435, fax: ++386-22527-774*

*Received: 03-03-2011*

## Abstract

Biogas is a mixture of gases produced by anaerobic fermentation where biomass or animal waste is decomposed and methane and carbon dioxide are mainly released. Biogas also has a very high moisture content (up to 80%), temperatures of around 60 °C, high pressure, and can contain other gases ($N_2$, $H_2S$, $NH_3$ and $H_2$). We searched for an appropriate measuring system for the determining of oxygen in biogas, since the production process of biogas must be run under anaerobic conditions; as the presence of oxygen decreases the quality of the biogas.

Ruthenium (II) complexes are by far the most widely-used oxygen dyes within optical oxygen sensors. In general, they have efficient luminescences, relatively long-life metal-ligand charge-transfer excited states, fast response times, strong visible absorptions, large Stokes shifts, and high-photochemical stability. The purpose of this work was to characterise and optimize an optical oxygen sensor using tris (4,7-diphenyl-1,10-phenanthroline) ruthenium(II) dichloride complex for measuring oxygen. Different sensor properties were additionally studied, focusing on the interference of external light, temperature, and various gases. A special gas-mixing chamber was developed for gas interference study, and on-line experiments are presented for oxygen determination within the pilot biogas reactor.

**Keywords:** Tris (4,7-diphenyl-1,10-phenanthroline) ruthenium(II) dichloride complex, oxygen optical sensor, interferences, biogas

## 1. Introduction

There is growing interest in the developement of new photochemical oxygen sensors and this trend has been greatly stimulate by the environmental pollution problem over the last two decades.[1] Several oxygen-detection systems have been reported based on redox titration, polarography or the measurement of chemiluminescence intensity.[2–4]

When determining oxygen, the classical Clark – type amperometric electrode, based on the electroreduction of oxygen on a polarized cathode, is still the dominate oxygen sensor.[5–6] Some of the limitations of Clark electrodes are well known, such as the consumption of oxygen and their relatively long response time. The Clark oxygen electrode is also limited by the stability of the electrode surface and by instabilities in the oxygen diffusion barrier.[5]

Therefore, a variety of different optical devices and sensors have been developed for measuring oxygen. They are immune to exterior electromagnetic field interference and can also be produced as disposable sensors. The latter

**Table 1:** Overview of luminescence dyes used for oxygen determination with excitation ($\lambda_{exc}$) and emission ($\lambda_{em}$) wavelength present.

| Dye | Support for immobilization | $\lambda_{exc/em}$ (nm) | $\Phi_L$ | $I_o/I_{100}$ |
|---|---|---|---|---|
| Pyrene-1-butylic acid | Poly(dimethylsiloxane) | 365/396 | | 1.50 |
| Ru(dpp)$3^{2+}$ | Silicone | 457/610 | 0.50 | 4.40 |
| | Polystyrene | 457/610 | 0.50 | 1.10 |
| | PVC | 457/610 | 0.50 | 3.50 |
| | Poly(dimethylsiloxane) | 457/610 | 0.50 | 4.50 |
| Re(I)L(CO)3CN+ | | | | |
| L = bpy | Silicone | 250/448 | 0.59 | 2.20 |
| L = phen | Silicone | 250/448 | 0.77 | 5.40 |
| L = Me4phen | Silicone | 274/462 | 0.68 | 41.00 |
| Os(dpp) $3^{2+}$ | Poly(dimethylsiloxane) | 502/729 | – | 4.50 |
| Ir(ppy)3 | Polystyrene | 376/512 | – | 15.30 |
| Platinum(II) octaethylporphyrin | Polystyrene | 535/646 | – | 4.50 |
| Platinum(II) tetrakis(pentafluorophenyl) porphyrin | Polystyrene | 508/648 | – | 3.00 |
| Platinum(II) tetrakis(pentafluorophenyl) porphyrin | Polystyrene | 508/648 | – | 3.00 |
| Platinum(II) octaethyl porphine ketone | PVC | 592/758 | 0.01 | 2.00 |
| | Polystyrene | 592/758 | | 20.0 |
| Palladium(II) octaethylporphyrin | Polystyrene | 546/663 | 0.12 | 11.50 |
| Palladium(II) octaethyl porphine ketone | PVC | 602/790 | 0.01 | 8.00 |
| | Polystyrene | 602/790 | – | 28.00 |
| Aluminum tetraphenoxy PcOH | Polystyrene | 606/705 | – | 1.00 |
| (dppe)Pt{$S_2C_2$($CH_2CH_2$N-2-pyridinium) | Cellulose acetate | 470/710 | 0.01 | 2.50 |
| Aluminum ferron | Sol gel (TMOS and MTMOS) | 380/5/80 | – | 5.00 |

*Abbreviations:* $\Phi_L$ = the luminescence quantum yield, $I_o/I_{100}$= Stern-Volmer plot, dpp = 4,7-diphenyl-1,10-phenanthroline, bpy = 2,2-bipyridine, phen = 1,10-phenanthroline, Me4phen = tetramethyl-1,10-phenanthroline, t-Bu = tetrabuthyl, ppy = 2-phenylpyridine anion, PcOH = phthalocyanine hydroxide, dppe = 1,2-bis(diphenylphosphino)ethane, ferron = 8-hydroxy-7-iodo-5- quinolinesulfonic acid, TMOS = tetramethoxysilane, MTMOS = methyltrimethoxysilane.

two properties are especially attractive when using these sensors during biotechnology, and in disposable microbioreactors.[7–8] These optical devices are based on the luminescence quenching of organometallic complexes by paramagnetic oxygen.[5] Table 1 presents an overview of luminescence dyes used for the determination of oxygen.[7,9–20]

In order to determine the concentration of oxygen within a local-small or micro environment, it is important that the instruments measuring area is minimal and easy to use. In this case optical-fibre sensors prove to be the most appropriate.[21] Conventional measurement systems based on electrochemical methods are susceptible to several limitations: they show an inherent oxygen consumption, are influenced by sample flow-rate or stirring speed, are cross-sensitive to $CO_2$ and $H_2S$, and fouling of the membrane can also present a severe problem. Optical sensors do not have these disadvantages and, therefore, present a realistic alternative to electrochemical methods.[21–23]

Optical oxygen sensors are also more attractive than conventional amperometric devices due to their: faster response time, high sensitivity and selectivity, no oxygen consumption, no surface poisoning, and no positioning of an additional reference electrode.[22] Usually, the optical film of an optical sensor (optode) consists of an analyte-sensitive dye and a support matrix in which the dye is dispersed or dissolved.[24] The most commonly-used are polycyclic aromatic dyes or metal complexes dispersed within an oxygen permeable polymer. Two general types of oxygen sensitive dyes have been introduced so far. The first are polycyclic aromatic hydrocarbons and porphyrins such as pyrenebutyric acid, perylene dibutyrate, pyrene/perylene, 9,10-diphenylanthracene, decacylen and tetraphenylporphyrin. The latter are metallorganic complexes including ruthenium(II) complexes, platinum(II) complexes or porphyrins, palladium(II) porphyrins, rhenium(I) complexes, osmium(II) complexes, gold(I) complexes, lead(II) complexes [11] and an aluminium (III) complex.[24]

Ruthenium (II) complexes are by far the most widely-used oxygen dyes because these complexes, in general, have efficient luminescences, relatively long-life metal-ligand charge-transfer excited states, fast response times, strong visible absorptions, large Stokes shifts, and high photochemical stability. Furthermore, the long excitation and emission wavelengths are more compatible with solid state opto-electronic monitoring technology.[23, 25]

The quenching process of $Ru^{II}$ in the presence of oxygen can be expressed as follows:

$$Ru^{II*} + O_2 \rightarrow Ru^{II} + O_2^{\ *} \quad (1)$$

where $Ru^{II}$ denotes the complex and »*« denotes its excited state. [25]

The basic operational principle of a fluorescent optical sensor for measuring oxygen is based on reducing the intensity of fluorescence (quenching) due to the involvement of oxygen in the dye's structure. The calibration of most luminescence quenching-based optical sensors, relies in essence on the Stern-Volmer equation.[26] Ru(II) complexes exhibit high sensibility to luminscence quenching and the position of their absorption and emission spectra permits the application of low-cost, solid-state optoelectronics for the detection of luminescence intensity: the dyes can be excited with blue or even blue-green light-emitting diodes (LEDs) and exhibit large Stokes shift, resulting in the emission of orange-red light.[27] In the past, as part of the optochemical detection system for oxygen, dye – Ru $(phen)_3$ was introduced for the simultaneous measurement of pH, carbon dioxide and oxygen.[28]

In this present work, dye – tris (4,7-diphenyl-1,10-phenanthroline) ruthenium(II) dichloride complex was used for the preparation of optical oxygen sensors. The presented sensor introduces many advantages: simple preparation and use, explosion-proof setup, measurements are possible during water or gas phases, and measurement in over or under pressure conditions. Different sensor properties were studied focusing on the interference of external light, temperature, and various gases. A special gas mixing chamber was developed for gas interference study since in the literature there are no similar systems or studies reported. Finally, preliminary experiments are presented for oxygen determination in a biogas reactor. Future works will focuse testing the sensor for oxygen within different environments (biogas and landfill gas analysis), biotechnology, and clinical applications.

# 2. Experimental

## 2. 1. Chemicals and Solutions

All the chemicals used were of analytical purity grade. All solutions were prepared with deionised water. Silicon (ElastosilE4, Wacker), polymer lyer (Folex-B72,A4), tris (4,7-diphenyl-1,10-phenanthroline) ruthenium(II) dichloride complex (Sigma Aldrich) and methilethilketone (Sigma Aldrich) were used for the sensor's preparation.

The following gases were used for examining the impact of various gases on an optical oxygen sensor: carbon dioxide ($CO_2$ 99.995%, Messer d.o.o.), carbon monoxide (CO in nitogen, 2000 ppm, Euro-gas Management Services Ltd), nitrogen oxide (NO in nitrogen, 1000 ppm, Euro-gas), nitrogen dioxide ($NO_2$ in air, 1000 ppm, Euro-gas Management Services Ltd), sulphur dioxide ($SO_2$ in nitrogen, 1000 ppm, Euro-gas Management Services Ltd), ammonia ($NH_3$ in nitrogen, 500 ppm, Euro-gas Management Services Ltd), methane ($CH_4$ 100%, Euro-gas Management Services Ltd) and nitrogen ($N_2$ 99.999%, Messer d.o.o.).

## 2. 2. Apparatus

Optical measurements were studied using: AvaSpec-2048 (Avantes) spectrophotometer, 200 μm optical fibre (Avantes), blue LED diode (RLS-5B475-S), $\lambda_{em}$= 477 – 480 nm (Roithner Lasertechnik), gas mixing chamber (Echo d.o.o.) and flow cell (R-Tehnika d.o.o.). Additional equipment used was: AB54-S balance (Mettler Toledo), power supply GPS-303OD Goodwill model and MST digital magnetic stirrer (Ika). Measurements of biogas were performed within a 120 L PVC pilot reactor with an additional temperature sensor (Visidaq-Genie, Professional V3).

## 2. 3. Preparation of Tris (4,7-diphenyl-1, 10-phenanthroline) Ruthenium(II) Dichloride Optical Oxygen Sensors

The sensor solution was prepared from 45.4 mg tris (4,7-diphenyl-1,10-phenanthroline) ruthenium(II) dichloride complex diluted in 10 mL of methylethylkethone. The prepared sensor solution was mixed on magnetic stirrer for about 3 h, until the ruthenium complex was completely dissolved. 1.05 g of silicone was added to 4 mL of sensor solution and the prepared mixture was stirred for 3 h at 80 °C. After most of the solvent had evaporated and the sensor solution became very homogeneous and viscous, it was transferred onto a transparent PVC holder – 100 μm film Folex (Figure 1). Then the prepared optical sensors were dried for 48 h at room temperature of (25 ± 1 °C). After drying, the optical sensors were cut to the dimensions of 1.75 $cm^2$ – 15 mm in diameter. The sensors were stored in a dark and dry place before use.

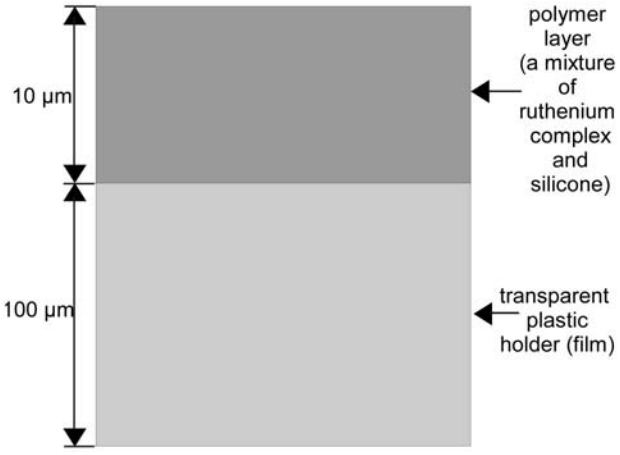


**Figure 1:** Schematic picture of an optical oxygen sensor.

## 2. 4. Measurement Procedures

A blue LED diode was used as a light source and was switched on for 60 min to achieve stable conditions

**Figure 4:** Optical oxygen sensor, positioning under the 45° angle.

before each measurement. The current through the LED diode was controlled by a power supply which operated at a constant current I = 6.35 A, (λ = 575 nm).

A spectrophotometer was used for the analysis of excitation and emission light spectra. A fibre containing six 200 μm optical fibres was used for transfering the optical signal, 200 μm optical fibres were used for illumination. Sufficiently excitation intensity and high measuring signal was achieved using these optical fibres. A complete spectrum from 350 to 1000 nm was measured for the excitation and emission fluorescence signal.

As a carrier gas nitrogen was used the callibrations of the optical oxygen sensor were performed at 0, 25, 50, 75 and 100% oxygen concentrations. Several different gas mixtures for investigating interferences when measuring oxygen ($CO_2$, CO, NO, $NO_2$, $SO_2$, $NH_3$ and $CH_4$) (Table 2) were prepared with the use of a gas-mixing chamber. During the constant flow of the carrier, gases in different concentrations were added, and precise gas mixtures were prepared within the range from 1.0 to 1000.0 ppm with ± 0.7 ppm accuracy (repeatability ± 0.15%, the full scale including linearity was from 15 to 25 °C and from 70 to 400 kPa). Figure 2 schematically present the system used for optical measurements. Sensor calibration and interference studies were preformed using the described system.

**Table 2:** Concentrations and types of gases exposed to the optical oxygen sensor.

| GAS | *c* (ppm, %) |
|---|---|
| Carbon monoxide (CO) | 1000 ppm |
| Carbon dioxide ($CO_2$) | 50.0% |
| Nitrogen oxide (NO) | 500 ppm |
| Nitrogen dioxide ($NO_2$) | 500 ppm |
| Sulfur dioxde ($SO_2$) | 500 ppm |
| Ammonia ($NH_3$) | 250 ppm |
| Methan ($CH_4$) | 50.0% |

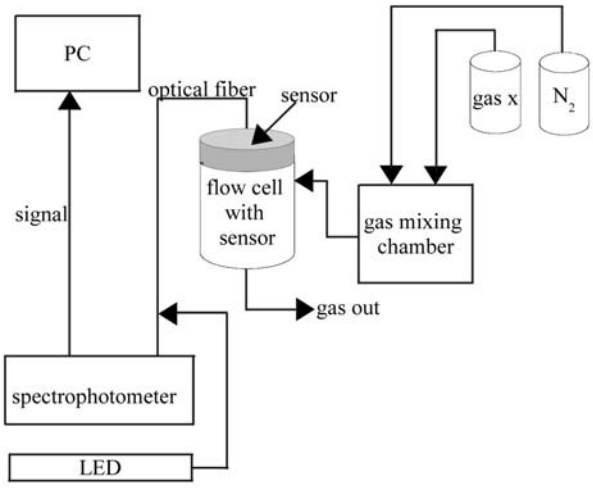


**Figure 2:** System used for optical measurements.

Figure 3 demonstrates the positioning of the optical oxygen sensor within the optical probe, where the sensors (15 mm in diameter) were placed at the end of the probe within a flow-through cell. Firstly, the sensor was excited when the blue LED light was below the 180° angle. Acarrier-gas was supplied with a flow-rate of 1.0 L/min at the top of the flow-cell (the exit was freely opened and there was no over-pressure in the measuring cell).

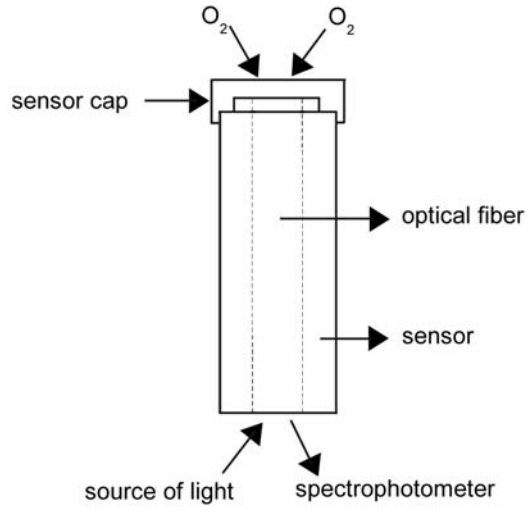


**Figure 3:** Scheme of the optical probe with the optical oxygen sensor.

Additionaly, the sensor was placed and positioned so that the light of the blue LED diode falled when the oxygen sensor was under the 45° angle (Figure 4). The entire system was then placed into a black air-tight 40 mL polypropylene container. The container protects the sensor from external light, but had two connectors for in and out-coming gas. The measurements were preformed at room temperature 20 ± 1 °C and atmospheric pressure of 95 ± 5 kPa. The influences of various gases on the oxygen sensor was studied by changing the gas concentrations within the mixing chamber.

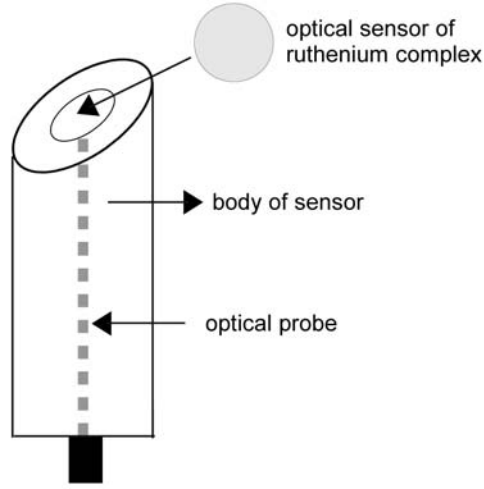

## 2. 5. Real Time Determination of Oxygen in a Biogas Reactor

The aim of this work was to study the digestion system in a pilot scale bioreactor (120 L) with leachate recirculation and pH adjustment, using green residue as feedstock. The digester operated within a thermophilic range (49–59 °C), under dry conditions. The sensor was tested in a pilot reactor for the determination of oxygen whilst biogas was produced. The pilot reactor was covered with gas – tight PVC plates, sealed with rubber, and heated to the thermophilic level. The temperature was additionally-controlled (55 ± 3 °C). The reactor was additionally-insulated from the outside in order to obviate heat loss. Green residue was obtained from the Čisto mesto landfill in Ptuj, Slovenia, and contained wood biomass, consisting of tree and shrub prunings and old wood. A large part of this green residue consisted of grass cuttings, hedge trimmings, old flowers, weeds, and leaves. The green residue also contained food waste, mainly raw vegetable and fruit waste-matter (the chemical feedstock analysis is shown in Table 3). The feedstock for the reactor (green residue) was chopped into particle sizes of less than 5 cm, and added to the reactor. The reactor contained 42.5 kg of material. The green residue was first treated aerobically and then anaerobically. After sealing the gas-tight lids of the reactor, hot air was used (1 h) for reactor ventilation. In this way, the substrate was aerated and aerobic microbiological activity caused an increase in temperature. During this aerobic phase, the temperature reached 60 ± 2 °C.

The concentration of oxygen was measured within the upper-head space of the bioreactor during 20 days of biogas production over ananaerobic phase (Figure 5). Temperature and humidity were also controlled during the biogas production. The optical oxygen sensor was connected on-line to the spectrophotometer, and the whole process was carried out in darkness.

# 3. Results and Discussion

## 3. 1. Tris (4,7-diphenyl-1,10-phenanthroline) Ruthenium(II) Dichloride Optical Oxygen Sensor's Properties

The concentration of dye –tris (4,7-diphenyl-1,10-phenanthroline) ruthenium(II) dichloride complex was optimized first. The optimal sensitivity for the optical oxygen sensor was at 4.9 mg/L for ruthenium complex concentrations. In the case of lower concentrations of the dye, the optical signal must be additionally-amplified–in addition amplification automatically increases the noise signal of the measuring system. Oppositely, the solubility of the dye in methilethilketone was limited, when the concentrations of ruthenium complex were higher, therefore non-homogeneous solutions, including bigger particles, were formed resulting in an uneven thickness of the sensor's surface. The Stern-Volmer equation[26] describes the interaction between fluorescence intensity and the concentration of the analyte. The homogene polymeric matrix

**Table 3:** The chemical feedstock analysis including moisture, combustion residue, pH, total Kjeldahl nitrogen (TKN), and total organic carbon (TOC).

| | Moisture (%) | Comb. res. (% d.w.) | pH | TKN (% d.w.) | TOC (% d.w.) |
|---|---|---|---|---|---|
| **Green residue (input substr.)** | 49± 10 | 41 ± 3 | 7.3 ± 1.0 | 1.5 ± 1.0 | 19± 2 |

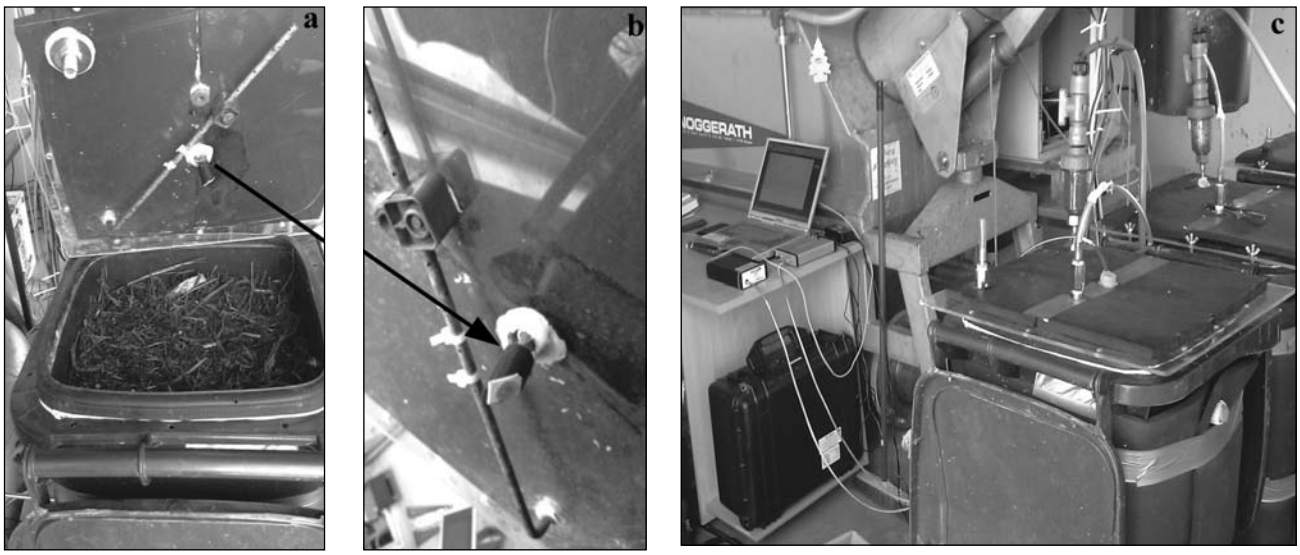


**Figure 5:** Positioning of the optical oxygen sensor (a, b)within the pilot bioreactor (c).

directly affects the Stern-Volmer linearity. Defining dye surrounding – the voids and polymer particles, is crucial for stable sensor response, and this is also the main reason why all the presented molecules (Table 1) are unequally good indicators for oxygen. The decline of fluorescence is also highly-dependent on the diffusion and solubility of the oxygen, adsorption the dye in the polymer matrix.

A transparent PVC holder (100 μm film Folex) was used for sensor preparation and has several advantages vs. glass or other sol-gel holders since it is flexible, very easy to cut and modify thus allowing preparation of different shapes and areas of Ru-sensors, and is also a very accessible low-cost holder.

Figures 6 and 7 present the sensor responses to oxygen using the described optical oxygen sensors. The sensor was exposed to various concentrations of oxygen at different incident light angles of 45° (Figure 6) and 180° (Figure 7). In particular, the impact angle of the LED light (475 nm) falling onto the sensor's surface was studied, where the emitting maximum light was at 596.22 nm. Different concentrations of oxygen were prepared within the mixing chamber, from oxygen and pure nitrogen at T = 19°C, p = 98 kPa, the other conditions being described in Chapter 2.4. Excitation light-intensity was constant, the intensity of fluorescence changed depended on oxygen concentration. Figures 6 and 7 have the same form, no deviations were detected, on both figures the lowest fluorescence emission intensity was at 100% oxygen and the maximal fluorescence emission intensity at 100% nitrogen. Oxygen was incorporated into the structure of the tris (4,7-diphenyl-1,10-phenanthroline) ruthenium(II) dichloride complex where it acts as an quencher. Sensor sensitivity at the 45° angle was approximately 50 times higher than at the 180° angle, the increase in sensitivity resulting from better diffussion in the polymer layer and longer contact time at a 45° incident light angle.

The stability of the sensors was tested and the sensors exposed to external light source (200–800 nm), T = 20 ± 2 °C for 21 days. Figure 8 shows that the sensor's response decreases with time when exposure to external light. The response of the sensor after 5 days of exposure to external light had already reduced by about 70%, and after 21 days by approximately 80%. Constant and long-term exposure of tris (4,7-diphenyl-1,10-phenanthroline) ruthenium(II) dichloride complex to external light decomposses the dye, therefore the sensors were additionally-protected by positioning them in a black polypropylene air-tight container. Short-term measurements were preformed using a frequency-modulated source, and by introdu-

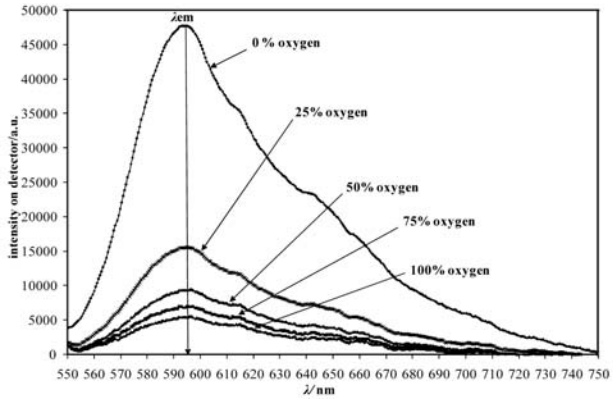


**Figure 6:** Optical oxygen sensor response for various oxygen concentrations (45° angle).

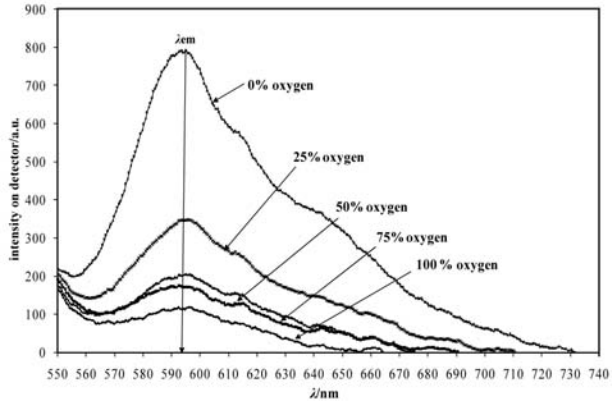


**Figure 7:** Optical oxygen sensor response for various oxygen concentrations (180° angle).

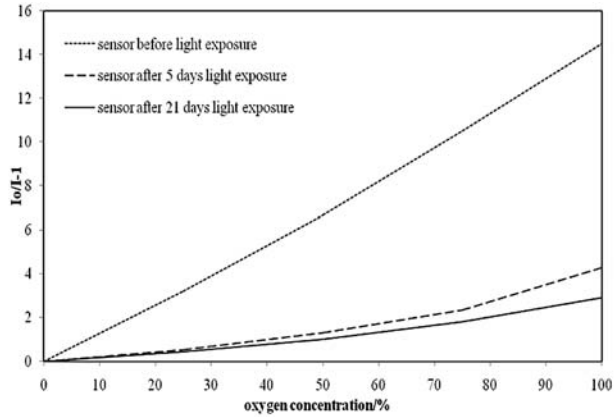


**Figure 8:** Effect of external light source (200–800 nm) to the optical oygen sensor.

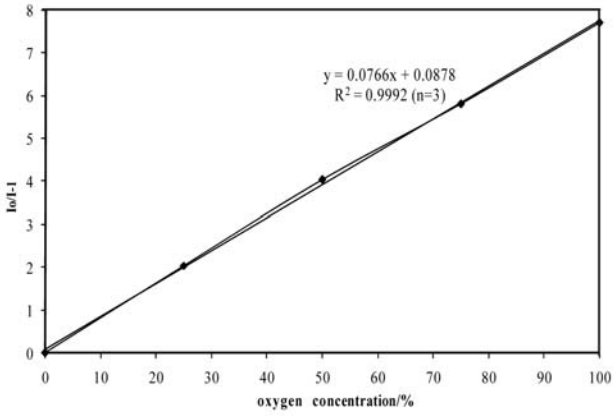


**Figure 9:** Calibration curve for oxygen using optical oxygen sensor (n = 3).

cing regular calibration of the sensor in order to improve and prolong the life-times of the sensors. Figure 9 present the calibration curve for optical oxygen sensor (n = 3) at 0, 25, 50, 75 and 100% oxygen concentrations in nitrogen. The calibration curve was linear ($R^2$ = 0.9992) within the whole measured region (y = 0.0766x + 0.0878).

## 3. 2. Interference Study of Different Gases on Optical Oxygen Sensor Properties

The interferences of different gases were studied using a gas-mixing chamber and the described optical oxygen sensor. CO, $CO_2$, $CH_4$ and $NH_3$with the corresponding concentrations (Table 2) where selected according to their potential concentrations in the biogas. During the first step, the whole spectral-range was observed in order to compare deviations or any other spectral changes concerning interference. NO, $NO_2$ and $SO_2$where additional tested, since their influence on the optical oxygen sensor can be important for other applications, although relevant data is absent in the literature.

Figure 10 presents the influence of CO, $CO_2$, $CH_4$, and $NH_3$ on the optical oxygen sensor. First the sensor was exposed to 100% $N_2$ (flow = 1.0 L/min) for 2 minutes. Then interference gas was added and after two minutes of purging the sensor was again exposed to 100% $N_2$. The whole procedure was repeated six times. It is evident from Figure 10 that CO, $CO_2$, $CH_4$ and $NH_3$ did not have any effect on optical oxygen sensor's response.

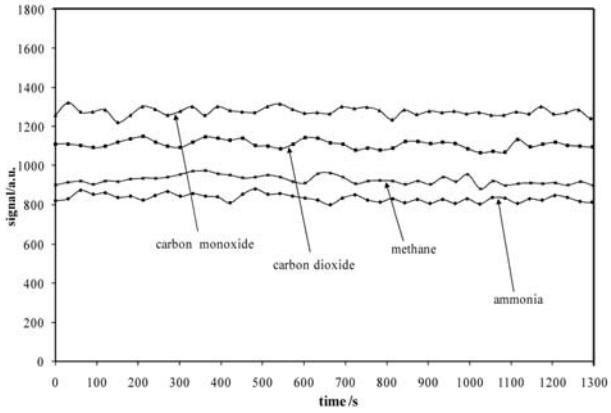


**Figure 10:** The influence of CO, $CO_2$, $CH_4$, and $NH_3$ on the optical oxygen sensor.

Figure 11 present the exposure of $NO_2$ to the optical oxygen sensor. First, the sensor was exposed to 100% $N_2$ (flow = 1.0 L/min) for 2 minutes, then $NO_2$ was added in a 500 ppm concentration. After two minutes of purging with nitrogen, the procedure was repeated six times (two cycles were present). Each $NO_2$ addition reduced the measured signal and the baseline signal decreased (in the first cycle by 20% and in the second cycle by 25%). The interference effect of NO in a 500 ppm concentration, gave us the same result. The interference of NO and $NO_2$ was irreversible, probably resulting from the decomposition-oxidation of the dye. Further studies are planned for investigating the phenomena, and its mechanism.

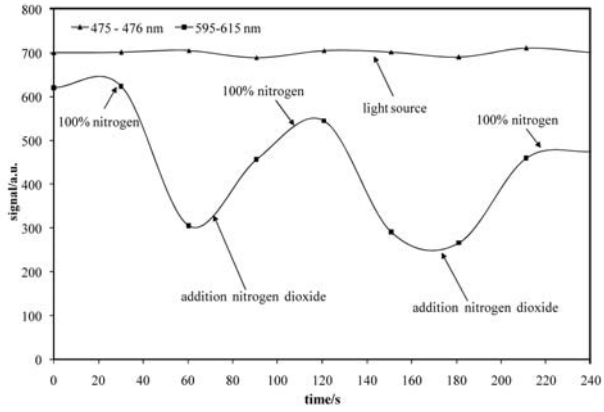


**Figure 11:** The influence of $NO_2$ on the optical oxygen sensor.

Figure 12 present the exposure of $SO_2$ to the optical oxygen sensor. First, the sensor was exposed to 100% $N_2$ (flow = 1.0 L/min) for 2 minutes, then $SO_2$ was added in a 500 ppm concentration. After two minutes of purging with nitrogen, the procedure was repeated six times (four cycles were present). Each $SO_2$ addition reduced the measured signal by arround 50% but the baseline signal returned to its original value. The interference, compared to the NO or $NO_2$ effect, was different and is reversible, resulting from $SO_2$ incorporation within the dye, where $SO_2$ acts as a fluorescence quencher similar too xygen. From the results, NO, $NO_2$, and $SO_2$ present interference for oxygen sensing but this could be solved, in practice using on-line positioning of commercially-available air filters.

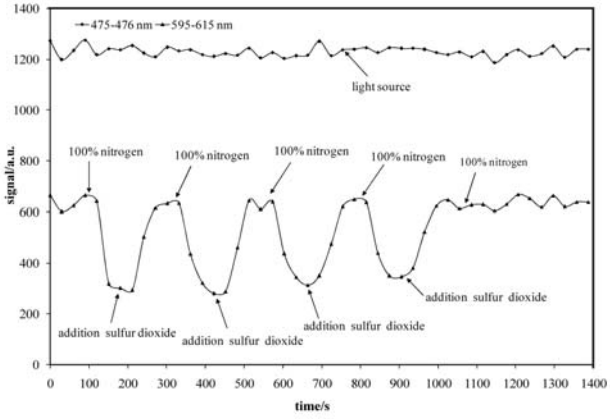


**Figure 12:** The influence of $SO_2$ on the optical oxygen sensor.

## 3. 3. Application of a Sensor Within the Biogas Reactor

The concentration of oxygen was measured within the bioreactor over 20 days of anaerobic biogas produc-

tion (Figure 13). The external oxygen concentration was 20.5%, and the avarage temperature during the process was 54 ± 2°C. When the pilot reactor was closed, the concentration of oxygen fell to 16% in one day. The lowest –0.2% concentration of oxygen was measured after 8 days, and coincided with an $CH_4$ increase. At that time the concentration of $CH_4$ was 27%, the $CO_2$ concentration 61%, and the $N_2$ concentration11%. The concentrations of CO and $H_2S$ were also measured and were at the 200 ppm level. The concentration of $CH_4$ reached a constant value (27%, day 8), therefore the bioreactor was quickly opened, and the green residue sampled for chemical analysis. An increase in the oxygen concentration of up to 6% was detected at that time, and was a result of external oxygen impact. Chemical analysis of the green residue in the bioreactor after 8 days of fermentation suggests that approximately 13% of biomass was decomposed in comparison to the data presented in Table 3. The constant –0.4% concentration of oxygen was measured after 10 days, and up to the end of the experiment. During this period biogas was produced with a composition of: $CH_4$(27–30%), $CO_2$ (47–61%), and $N_2$ (11–22%), the concentrations of CO and $H_2S$ being below 150 ppm.

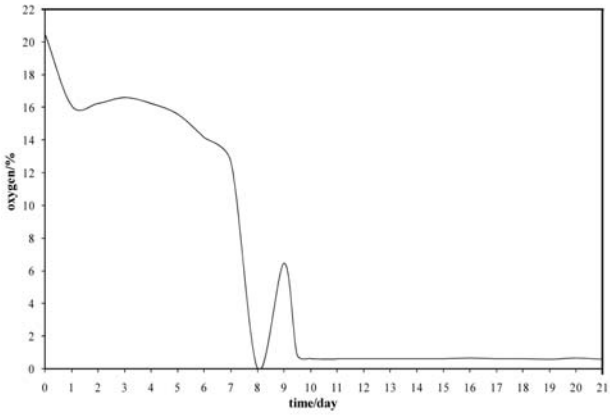


**Figure 13:** Concentration of oxygen in the pilot bioreactor versus time.

## 4. Conclusions

Despite numerous published articles, there are in practice still many uncertainties regarding the use of an optical oxygen sensor using a tris (4,7-diphenyl-1,10-phenanthroline) ruthenium(II) dichloride complex.

The optimal sensitivity of the optical oxygen sensor present was at a 4.9 mg/L ruthenium complex concentration. The defining dye surrounding – the voids and polymer particles, was crucial for stable sensor response, whilst the decline in fluorescence was also highly-dependent on the diffusion and solubility of the oxygen, and the adsorption of the dye within the polymer matrix. Sensor sensitivity was increased by positioning the sensor at a 45° angle (it was approximately 50 times higher than at the 180° angle), an increase in sensitivity then resulting from better diffussion within the polymer layer, and a longer contact time. The optical oxygen sensor responded to 0, 25, 50, 75 and 100% oxygen concentrations in nitrogen linear ($R^2$ = 0.9992), throughout the whole measured region (y = 0.0766x + 0.0878).

The interferences of different gases were studied regarding the optical oxygen sensor's response. CO, $CO_2$, $CH_4$ and $NH_3$ did not have any significant impact, whereas NO and $NO_2$ presented irreversible and $SO_2$-reversible effects– where $SO_2$ was, similarly to oxygen incorporated within the dye, as a quencher.

Finally, using experiments within the bioreactor, we demonstrated that the optical oxygen sensor is appropriate for measuring the oxygen in biogas. The presented sensor has the following advantages: it is easy to use and allows measurements in water or during gaseous phases, has an explosion-proof setup, and can do measurements in wells where negative pressure or overpressure of gas are possible.

## 5. Acknowledgements

The authors would like to thank the Slovenian Technology Agency (TIA) for the financial support through Grant P-MR-08/54.

The financial support of the Slovenian Ministry of Higher Education, Science and Technology (contract 3211-10-000057) is also acknowledged.

## 6. References

1. H. Zhang, B. Li, B. Lei, W. Li, *J. Lumin.* **2008**, *128*, 1331–1338.
2. L. C. Clark, US Patent Number 2, 913, 386, date of patent November 17, **1959**.
3. T. M. Freeman, W. R. Seitz, *Anal. Chem*. **1981**, *53*, 98–105.
4. M. C. Hitchman, Measurement of Dissolved Oxygen, Wiley, New York, **1978**, pp. 130–132.
5. J. F. Fernandez-Sanchez, T. Roth, R. Cannas, Md. K. Nazeeruddin, S. Spichiger, M. Graetzel, *Talanta.* **2007**, *71*, 242–250.
6. J. F. Fernandez-Sanchez, R. Cannas, S. Spichiger, R. Steiger, U. E. Spichiger-Keller, *Anal. Chim. Acta.* **2006,** *566*, 271–282.
7. Y. Kostov, G. Rao, *Sensor. Actuat. B-Chem.* **2003**, *90*, 139–142.
8. S. Arain, G. T. John, C. Krause, J. Gerlach, O. S. Wolfbeis, I. Klimant, *Sensor. Actuat. B-Chem.* **2006**, *113*,639–648.
9. Y. Amao, *Microchip. Acta.* **2003**, *143*, 1–12.
10. A. Sharma, O. S. Wolfbeis, *Appl. Spect*. **1998**, *42*, 1009–1011.
11. L. Sacksteder, J. N. Demas, B. A. DeGraff, *Anal. Chem*. **1993**, *65*, 3480–3483.

12. W. Y. Xu, K.A. Kneas, J. N. Demas, B. A. DeGraff, *Anal. Chem*. **1996**, *68*, 2605–2609.
13. Y. Amao, Y. Ishikawa, I. Okura, *Anal. Chim. Acta,* **2001**, *445*, 177–182.
14. S. K. Lee, I. Okura, *Spectrochim. Acta.* **1998**, *A 54*, 91–100.
15. S. K. Lee, I. Okura, *Anal. Commun*. **1997**, *34*, 185–188.
16. P. Hartmann, W. Trettnak, *Anal. Chem*. **1996**, *68*, 2615–2620.
17. D .B. Papkovsky, G. V. Ponomarev, W. Trettnak, P. O' Leary, *Anal. Chem*. **1995**, *67*, 4112–4117.
18. Y. Amao, T. Miyashita, I. Okura, *J. Porous. Media.* **2001**, *5*, 433–438.
19. Y. Amao, K. Asai, I. Okura, *Anal. Chim. Acta.* **2000**, *407*, 41–44.
20. J.M. Costa-Fernandez, M. E. Diaz-Garcia, A. Sanz-Medel, *Anal. Chim. Acta.* **1998**, *360*, 17–26.
21. W. Trettnak, W. Gruber , F. Reininger, I. Klimant, *Sensor. Actuat. B-Chem.* **1995**, *29*, 219–225.
22. H. Zhang , B. Li , B. Lei, W. Li, S. Lu, *Sensor. Actuat. B-Chem.* **2007**, *123*, 508–515.
23. P. Hartmann, M. J.P. Leiner, P. Kohlbacher, *Sensor. Actuat. B-Chem.* **1998,** *51*, 196–202.
24. M. M. F. Choi, D. Xiao, *Anal. Chim. Acta.* **1999**, *387*, 197–205.
25. X. Wu, L. Song, B. Li, Y. Liu, *J. Lumin.* **2010**, *130*, 374–379.
26. D. R. Walt, S.M. Bernard, US Patent Number 5, 244, 636, date of patent September 14, **1993**.
27. P. Hartmann, M. J. P. Leiner, M. E. Lippitsch, *Sensor. Actuat. B-Chem.* **1995**, *29*, 251–257.
28. M. M. F. Choi, D. Xiao, *Anal. Chim. Acta.* **2000**, *403*, 57–65.

## Povzetek

V prispevku predstavljamo optični senzor za določanje kisika, ki smo ga pripravili z nanosom tri (4,7 difenil-1,10-fenantrolin) rutenijevega(II) diklorida na PVC film. Občutljivost senzorja smo dodatno izboljšali s postavitvijo senzorja pod kotom 45°, zaradi povečane difuzije kisika in daljšega kontaktnega časa, v primerjavi s klasično postavitvijo senzorja pod kotom 180°. Optični senzor za določanje kisika se linearno odziva na 0, 25, 50, 75 in 100 % kisika v dušiku ($R^2$ = 0.9992, n = 3), znotraj celotnega koncentracijskega območja (y = 0.0766x + 0.0878).
Interferenčne študije plinov so pokazale, da plini, ki so prisotni v bioplinu ne motijo meritev, prav tako smo uspešno izvedli preliminarne meritve kisika v bioreaktorju. Razviti optični senzor za določanje kisika odlikuje enostavna uporaba, merjenje v nad in podtlačnih pogojih ter v plinastih in vodnih fazah.